Jpn. J. Appl. Phys. Vol. 42 (2003) pp. 3526–3527
Part 1, No. 6A, June 2003

Short Note

Ce–O Hybridization Effect of Protonic Conductor $SrCe_{1-x}Y_xO_{3-\delta}$ Observed by Resonant-Photoemission Spectroscopy

Tohru HIGUCHI, Takeyo TSUKAMOTO, Shu YAMAGUCHI[1], Noriko SATA[2*], Mareo ISHIGAME[2†] and Shik SHIN[3,4]

Department of Applied Physics, Tokyo University of Science, Tokyo 162-8601, Japan
[1]*Department of Materials Science, University of Tokyo, Tokyo 113-8656, Japan*
[2]*Institute of Multidisciplinary Research for Advanced Materials, Research Building of Scientific Measurements, Tohoku University, Sendai 980-8577, Japan*
[3]*Institute for Solid State Physics, University of Tokyo, Chiba 277-8581, Japan*
[4]*RIKEN, Hyogo 679-5143, Japan*

(Received November 28, 2002; accepted for publication February 17, 2003)

The Ce–O hybridization effect of protonic conductor Y^{3+}-doped $SrCeO_3$ ($SrCe_{1-x}Y_xO_{3-\delta}$) has been studied by resonant-photoemission spectroscopy (RPES). The RPES spectra show that the Ce $4f$ partial density of states in the valence band increases with increasing Y^{3+} dopant concentration. This finding indicates that the hybridization effect between the Ce $4f$ and O $2p$ states increases with Y^{3+} dopant concentration. [DOI: 10.1143/JJAP.42.3526]

KEYWORDS: $SrCe_{1-x}Y_xO_{3-\delta}$, protonic conductor, hybridization effect, electronic structure, resonant-photoemission spectroscopy (RPES)

Some perovskite-type oxides, such as $SrCeO_3$, $SrZrO_3$ and $SrTiO_3$, exhibit high protonic conductivity at sufficiently high temperature region when doped with acceptor ions.[1–6] They are important materials for a wide range of electrochemical applications, such as hydrogen fuel cells and sensors.[7] Theoretical and experimental investigations of the mechanism of proton migration have been reported in perovskite-type protonic conductors.[1–14] In Y^{3+}-doped $SrCeO_3$ and Sc^{3+}-doped $SrTiO_3$, the frequency of the O–H stretching vibration is found in the infrared transmission measurements,[2,5] indicating proton migration in the bulk state. Furthermore, the neutron diffraction indicates that the proton is bound by oxygen ions as if the proton makes the hydrogen bond between two oxygen ions. This fact is also supported from an *ab-initio* molecular-dynamics simulation.[12–14] Then, it is proposed that the proton migrates by hopping from site to site around the oxygen ion.

In recent years, the electronic structure of protonic conductor Sc-doped $SrTiO_3$ has been studied by optical absorption spectroscopy and resonant-photoemission spectroscopy (RPES).[8,9] The energy shift of absorption edge due to Sc doping is observed. The Fermi level shifts to the valence band side with increasing Sc dopant concentration. These behaviors are in good agreement with the rigid-band model. On the other hand, the RPES spectra show that the Ti $3d$ state hybridizes with the O $2p$ state in the valence band.[9] The hybridization effect depends on the Sc dopant concentration. Similar results have been reported for In-doped $CaZrO_3$.[10,11] Then, the authors suggested that the hybridization effect is closely related to the protonic conduction, though the contribution has not been clarified thus far.

In this study, the electronic structure of protonic conductor $SrCe_{1-x}Y_xO_{3-\delta}$ ($x = 0$, 0.05) has been investigated by RPES at the Ce $4d \rightarrow 4f$ absorption region. We discuss in this paper that the hybridization effect between the Ce $4f$ and O $2p$ depends on the Y^{3+} dopant concentration, as was previously observed in the case of $SrTi_{1-x}Sc_xO_3$.[9]

$SrCe_{1-x}Y_xO_{3-\delta}$ samples were sintered ceramics prepared by the solid-state reaction of $SrCO_3$, CeO_2, and Y_2O_3 at 1250°C, and pressed into cylinders of φ 13 mm × 80 mm, then sintered again in air at 1250°C for 20 h. The dopant concentrations were $x = 0$ and 0.05. The samples were confirmed as having a single phase with a perovskite structure by the powder X-ray diffraction analysis. The prepared samples were annealed in an atmosphere of N_2 vapor pressure at 800°C for 3 h in order to prevent protons from entering the crystal. In $SrCe_{0.95}Y_{0.05}O_3$, the electrical conductivities of dry-annealed and wet-annealed samples were $1.0 \times 10^{-10}\,\Omega^{-1}\mathrm{cm}^{-1}$ and $1.2 \times 10^{-10}\,\Omega^{-1}\mathrm{cm}^{-1}$, respectively, at 400°C. The activation energies (E_A) of dry-annealed and wet-annealed samples were 0.56 eV and 0.60 eV, respectively, at the temperatures below 500°C. The conductivity and E_A of $SrCeO_3$ were not determined. These values are in good agreement with the result of ref. 2.

RPES measurements were carried out at the revolver undulator beamline BL-19B at the Photon Factory of the High Energy Accelerator Organization, Tsukuba in Japan. Photoelectron energies were measured using an electrostatic hemispherical analyzer whose radius is 100 mm. The samples were scraped *in situ* with a diamond file in a vacuum of 3.0×10^{-10} Torr in order to obtain a clean surface. Since the $SrCe_{1-x}Y_xO_{3-\delta}$ has little conductivity at room temperature, the sample is charged. However, the sample has a finite conductivity at high temperature. Thus, the RPES measurement was carried out at 450 K to avoid the charging. The total-energy resolution was about 40 meV.

Figure 1 shows the constant-final-state (CFS) spectrum of $SrCe_{0.95}Y_{0.05}O_{3-\delta}$ obtained by collecting photoelectrons with a kinetic energy of 19 eV. This spectrum is regarded as the approximate absorption spectra of Ce $4d \rightarrow 4f$. The overall profile of the CFS spectra is similar to the $4d$ photoabsorption spectra of CeO_2 and $SrCeO_{3-\delta}$.[15,16] The vertical bars, which are labeled as ''on'' and ''off'', indicate the selected photon energies for the RPES measurements. The estimation of these excitation photon energies have been reported in refs. 15 and 16.

Figure 2(a) shows the RPES spectra of $SrCe_{1-x}Y_xO_{3-\delta}$ in the Ce $4d \rightarrow 4f$ energy region. The off-resonance spectra have two features α and β, which mainly consist of the O $2p$ state mixed with Ce $4f$ states. Comparing the off-resonance spectra, the intensity of α peak located at the top of the valence band is lower in $SrCe_{0.95}Y_{0.05}O_{3-\delta}$. In both on-

*Present address: Faculty of Engineering, Tohoku University, Sendai 980-8579, Japan.
†Present address: Akita Technical College, Akita 011-0923, Japan.

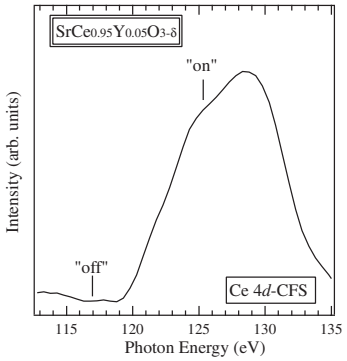

Fig. 1. CFS spectrum of $SrCe_{0.95}Y_{0.05}O_{3-\delta}$, corresponding to the Ce $4d \rightarrow 4f$ giant-absorption spectrum.

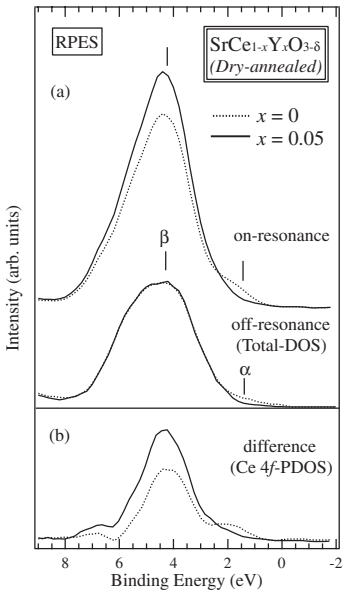

Fig. 2. (a) On- and off-resonance spectra of $SrCe_{1-x}Y_xO_{3-\delta}$ ($x = 0, 0.05$). The on- and off-resonance spectra were measured at $h\nu = 125.1$ eV and 117 eV, respectively. (b) Difference spectra obtained by subtracting the off-resonance spectra from the on-resonance spectra.

resonance spectra, the intensities of α and β peaks are enhanced by the Ce $4d \rightarrow 4f$ excitation. The resonance effect of β peak is stronger in $SrCe_{0.95}Y_{0.05}O_{3-\delta}$. The origin of the α peak will be discussed later.

Figure 2(b) shows the difference spectra by subtracting the off-resonance spectra from the on-resonance spectra. The difference spectra correspond to the Ce $4f$ partial-density of state (PDOS) in the valence band. Comparing the difference spectra, the Ce $4f$ PDOS is seen to be larger in the case of $SrCe_{0.95}Y_{0.05}O_{3-\delta}$. This fact implies that the hybridization effect between the Ce $4f$ state and O $2p$ state becomes more extensive with Y^{3+} dopant concentration, indicating that the bond length between Ce^{4+} and O^{2-} ions or the symmetry changes with a small amount of doping cations.

It is striking that the α peak is observed at the top of the valence band of $SrCeO_{3-\delta}$, though there is no peak at the top of the valence band of $SrCe_{0.95}Y_{0.05}O_{3-\delta}$. The existence of the α peak has been observed in a recent RPES study of fluorite-type oxide CeO_2 by Matsumoto and co-workers.[15,16] The Ce ion in $SrCeO_3$ is nominally tetravalent with no $4f$ electron such as that in CeO_2. The strength of the hybridization between the Ce $4f$ and O $2p$ states in the ground state of $SrCeO_3$ is similar to that in CeO_2. It is reported that the constant-initial-state (CIS) spectrum of the α peak has a maximum intensity at $\sim$122 eV, though the CIS spectrum of β peak has a maximum intensity at $\sim$125.1 eV.[15,16] This fact indicates that CeO_2 is mixed-valent between the $4f^0$ and $4f^1\underline{L}$ configurations in the ground states. Here, $\underline{L}$ denotes the hole in the valence band mainly composed of the O $2p$ state. Such a situation has also been observed in $SrCeO_{3-\delta}$. Therefore, we can ascribe the β peak to correspond to the Ce^{4+} state and the α peak to correspond to the Ce^{3+} state that exists on a sample surface or near an oxygen defect site. With a simple consideration, the hybridization between the $4f^0\underline{L}$ and $4f^1\underline{L}^2$ configurations in the final state is expected to nearly equal that between the $4f^0$ and $4f^1\underline{L}$ configurations in the ground state with the average $4f$ electron number of about 0.5. The average $4f$ electron number might decrease with Y^{3+} dopant concentration. Thus, the increase in the hybridization effect between the Ce $4f$ and O $2p$ states with Y^{3+} doping can be explained by the increase in the effective charges of Ce^{4+} and O^{2-} ions.

In conclusion, we measured the RPES spectra on protonic conductor $SrCe_{1-x}Y_xO_{3-\delta}$. The RPES spectra show that the hybridization effect between the Ce $4f$ and O $2p$ states increases with increasing Y^{3+} dopant concentration. This finding indicates that the effective charges of Ce^{4+} and O^{2-} ions decrease with Y^{3+} dopant concentration.

This work was partly supported by Sumitomo Foundation and a Grant-In-Aid for Scientific Research from the Ministry of Education, Culture, Sports, Science and Technology.

1) H. Iwahara, T. Esaka and H. Uchida: Solid State Ionics **3/4** (1981) 359.
2) S. Shin, H. H. Huang, M. Ishigame and H. Iwahara: Solid State Ionics **40/41** (1990) 910.
3) H. H. Huang, S. Shin and M. Ishigame: Solid State Ionics **47** (1991) 251.
4) T. Higuchi, T. Tsukamoto, N. Sata, K. Hiramoto, M. Ishigame and S. Shin: Jpn. J. Appl. Phys. **40** (2001) 4162.
5) N. Sata, K. Hiramoto, M. Ishigame, S. Hosoya, N. Niimura and S. Shin: Phys. Rev. B **54** (1996) 15795.
6) T. Higuchi, T. Tsukamoto, S. Yamaguchi, N. Sata, K. Hiramoto, M. Ishigame and S. Shin: Jpn. J. Appl. Phys. **41** (2002) 6440.
7) T. Yajima, K. Koide, N. Fukatsu, T. Ohashi and H. Iwahara: Sons. Actuat. B **13/14** (1993) 697.
8) T. Higuchi, T. Tsukamoto, N. Sata, M. Ishigame, Y. Tezuka and S. Shin: Phys. Rev. B **57** (1998) 6978.
9) T. Higuchi, T. Tsukamoto, N. Sata, M. Ishigame, Y. Tezuka and S. Shin: Solid State Ionics **108** (1998) 349.
10) T. Higuchi, T. Tsukamoto, Y. Tezuka, K. Kobayashi, S. Yamaguchi and S. Shin: Jpn. J. Appl. Phys. **39** (2000) L133.
11) S. Yamaguchi, K. Kobayashi, T. Higuchi, S. Shin and Y. Iguchi: Solid State Ionics **136–137** (2000) 305.
12) F. Shimojo, K. Hoshino and H. Okazaki: J. Phys. Soc. Jpn. **67** (1998) 2008.
13) F. Shimojo, K. Hoshino and H. Okazaki: J. Phys.: Condens. Matter. **10** (1998) 285.
14) F. Shimojo and K. Hoshino: Solid State Ionics **145** (2001) 421.
15) M. Matsumoto, K. Soda, K. Ichikawa, M. Kageyama, S. Tanaka, N. Sata, Y. Tezuka, S. Shin and O. Aita: J. Electron Spectrosc. Relat. Phenom. **78** (1996) 179.
16) M. Matsumoto, K. Soda, K. Ichikawa, S. Tanaka, Y. Taguchi, K. Jouda, O. Aita, Y. Tezuka and S. Shin: Phys. Rev. B **50** (1994) 11340.